Moving Receiver Tracking in Wireless Power Transfer Systems

Zhenzhe Han
Dept. of Engineering
University of Cambridge
Cambridge, UK
zh358@cam.ac.uk

Dai Jiang
Dept. of Electronic & Electrical Engineering
University College London
London, UK
d.jiang@ucl.ac.uk

Andreas Demosthenous
Dept. of Electronic & Electrical Engineering
University College London
London, UK
a.demosthenous@ucl.ac.uk

***Abstract*—Wireless power transfer (WPT) enables contactless power transfer from the power supply side coil (T_x) to the receiver side coil (R_x), which has a wide range of applications. However, for a horizontally randomly moving R_x, high power transfer efficiency (PTE) cannot be guaranteed as the relative distance between T_x and R_x affects the value of PTE. In this paper, we designed a 4-layer T_x array with R_x tracking algorithm to track the position of R_x and activate the T_x at that position in the array. Therefore, the maximal and stable PTE could be achieved for a freely moving R_x, which has been demonstrated in simulation experiments.**

***Index Terms*—moving R_x, PTE, R_x tracking algorithm, T_x array, WPT**

I. Introduction

Inductive WPT is a contactless power transfer technique through the mutual inductance of two coils, which is widely used in medical and industrial applications [1]. As shown in Fig. 1, a simple WPT system consists of a T_x coil as the power supply side and an R_x coil as the power receiver side. The equivalent circuit of the coil could be expressed by Fig. 2(b) [1]. The inductance of these two coils are indicated as L_1 and L_2 respectively, and the series loss of these two coils are resistors R_1 and R_2 respectively. The parasitic capacitance of both T_x and R_x could be neglected when the working frequency of WPT is much lower than the self-resonant frequency of T_x and R_x [1] [2]. Series capacitors C_1 and C_2 are used to realize resonance in the primary circuit and secondary circuit respectively. M is the mutual inductance coefficient. V_{in} is the input voltage and Z_{out} is the load. Power is transferred from the power supply to the load through mutual inductance of two coils.

In a dynamic WPT system, R_x is free to move on the horizontal plane. However, with a suitable load, PTE has strict requirements on the relative geometrical position of T_x and R_x. As shown in Fig. 2(a), the vertical distance between T_x and R_x is D and the lateral distance between T_x and R_x is Δ [1]. Under suitable and fixed D, the smaller the Δ, the higher the PTE [1] [3] [4] [5]. Under this condition, for a horizontally moving R_x, when T_x is fixed, PTE decreases as R_x moving away from T_x (Δ increases).

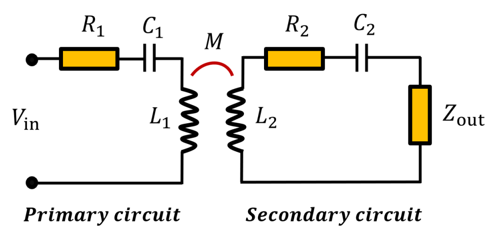

Fig. 1. WPT model.

To achieve maximal and stable PTE in the dynamic WPT system, we designed a T_x array system with a R_x tracking algorithm which could obtain the real-time location of moving R_x and activate the closest T_x coil in the T_x array. A maximal and stable PTE could be achieved in the dynamic WPT system by always keeping minimal Δ (with suitable D), which could realize stable wireless charging for moving devices.

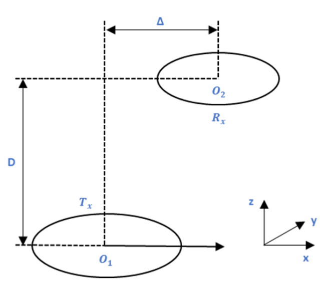

(a) Link model between two coils.

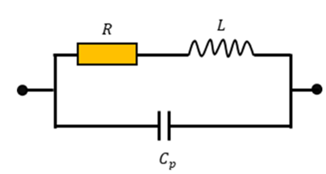

(b) Equivalent circuit for PCB coil.

Fig. 2. Coil modelling.

II. Methodology

A. Square Coil

PCB square coil was used in T_x array design. Fig. 3(a) shows the geometry structure of the PCB square coil [6].

The work was supported in part by the European Commission under Grant 824071 (NeuHeart) and in part by the Engineering and Physical Sciences Research Council under Grant EP/T001259/1 (PNEUMACRIT).

It is a square coil formed by a spirally coiled wire. Some important parameters are shown in Fig. 3(b) [1]. Fig. 2(b) shows an equivalent circuit of PCB square coil, which includes an inductor L with a series loss R and a parallel parasitic capacitor C_p between each track depending on the track spacing s [1].

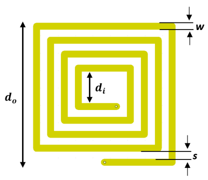

(a) Geometry structure.

Geometric		Electrical	
d_o	Outer Diameter	L	Inductance
l	Total Length	R	Series Loss
n	Number of Turns	Q	Quality Factor
d_i	Inner Diameter	C	Resonating Capacitance
w	Track Width	C_P	Parasitic Capacitance
s	Track Spacing	–	–

(b) Coil parameters.

Fig. 3. Square PCB coil.

B. T_x Array System

Fig. 4 shows the principle of the T_x array. Considering each square as a PCB square T_x spiral coil, R_x (red square) moves on T_x array freely. With a suitable vertical distance D between T_x and R_x, first a T_x is activated at $(1,2)^\mathsf{T}$ which is located exactly under R_x. When R_x moves away from $(1,2)^\mathsf{T}$ to $(2,1)^\mathsf{T}$, a R_x tracking algorithm could obtain the coordinates of T_x that R_x is located on, and activate this T_x ($(2,1)^\mathsf{T}$).

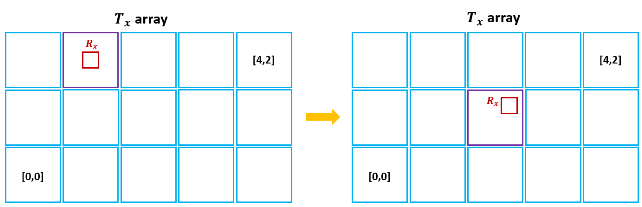

Fig. 4. Working principle of square T_x array.

R_x tracking algorithm tracks R_x by observing the change of coupling factor k. k is defined as:

$$k = \frac{M}{\sqrt{L_1 L_2}} \tag{1}$$

In Fig. 1, the PTE η equals to [7]:

$$\eta = \frac{P_{load}}{P_{in}} = \frac{(\omega_0 M)^2 Z_{\text{out}}}{(R_2 + Z_{\text{out}})\left\{R_1 (R_2 + Z_{\text{out}}) + (\omega_0 M)^2\right\}} \tag{2}$$

Under resonant frequency ω_0, for a certain load, the PTE achieves maximum when

$$k_{opt} = \sqrt{\frac{\left(\frac{Z_{\text{out}}}{R_2}\right)^2 - 1}{Q_1 Q_2}} \tag{3}$$

where $Q_{1,2} = \frac{\omega_0 L_{1,2}}{R_{1,2}}$ [7]. Therefore, we only need to find the optimal k to achieve maximal PTE. k_{opt} could be obtained by the geometry design of both T_x and R_x according to the load impedance Z_{out}. Fig. 5 shows that in Fig. 2(a), k and PTE have a similar downward trend as lateral distance Δ increases from zero when $k_{max} \leq k_{opt}$, which could be achieved by setting a suitable fixed vertical distance D. In this case, the position of R_x is the T_x coordinate that gives the maximal k in T_x array and this T_x coordinate could provide the maximal PTE.

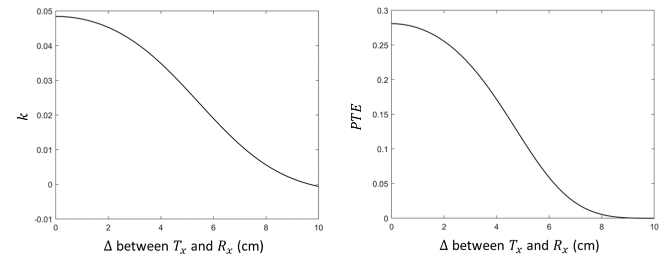

(a) k vs lateral distance Δ. (b) PTE vs lateral distance Δ.

Fig. 5. The relationship between k, PTE and Δ.

k in the topology described by Fig. 1 could be measured by using reflected impedance Z_{ref} in the primary circuit:

$$k = \sqrt{\frac{Z_{\text{ref}}\,(R_2 + Z_{\text{out}})}{L_1 L_2 \omega_0^2}} = \sqrt{\frac{\left(\frac{\dot{V}_{\text{in}}}{\dot{I}_1} - R_1\right)(R_2 + Z_{\text{out}})}{L_1 L_2 \omega_0^2}} \tag{4}$$

where $\dot{V}_{in}$ is the phase factor of input voltage and $\dot{I}_1$ is the phase factor of current in primary circuit.

However, a single layer T_x array cannot generate a stable k for moving R_x. As shown in Fig. 6, if R_x is located at the junction of each T_x coil (position 1, 2, 3), the coupling factor k at these locations would drop to an extremely low value no matter which coil is chosen. This is called weakly coupled region. An additional layer of T_x is added to compensate for these areas, so that R_x at locations 1, 2 and 3 are all located in T_x coil to provide a high coupling factor [8].

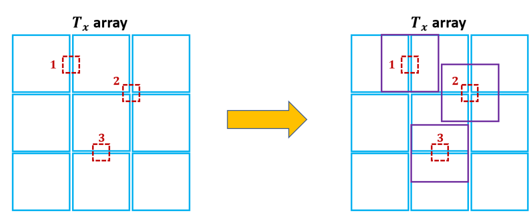

Fig. 6. The location (1,2,3) of R_x for low coupling factor k (weakly coupled region) & k compensation by using an additional layer of T_x.

A 4-layer square T_x array system was designed which covering all the compensation areas. Fig. 7 shows the design of a 5×3 4-layer square T_x array system. It contains four layers. The first layer is a normal 3×3 T_x array. The second layer is a 2×2 T_x array and it compensates for the location type 1 in Fig. 6. The third layer is a 1×3 T_x array and it compensates for the location type 3 in Fig. 6. The fourth layer is a 1×2 T_x array and it compensates for the location type 2 in Fig. 6. A 5×3 4-layer square T_x array can be obtained by stacking these layers vertically in order. Hence, the magnetic field coverage is more compact, which provides a more stable k for a moving R_x. As the T_x coils in each layer also experience mutual inductance, these T_x coils capture the otherwise lost magnetic energy and convert it into the induced current for secondary power transfer to R_x, which played a focusing role to improve k.

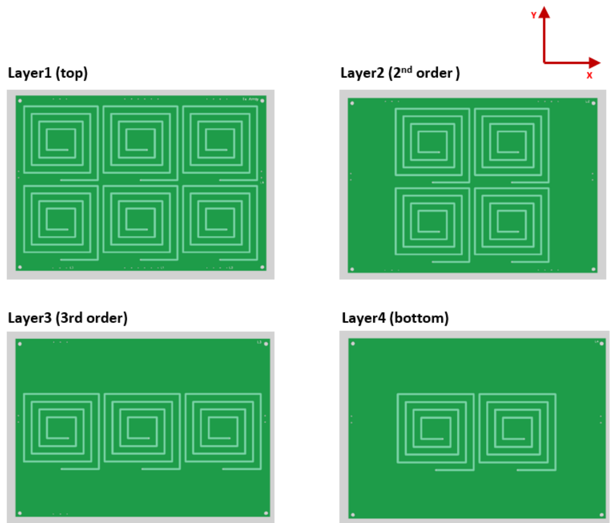

Fig. 7. Each layer of 4-layer square T_x array system.

Fig. 8 illustrates a way to construct a coordinate system for 4-layer T_x array, where 4 layers' vertical structure shows that the 4-layer T_x array is formed by stacking these four layers vertically. These four layers are represented by a different colours. Extracting the centre of each square T_x coil, a coordinate system could be obtained. Fig. 8 is a 5×5 4-layer T_x array system.

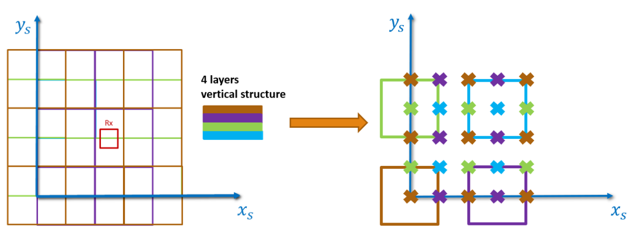

Fig. 8. The coordinate system of 4-layer T_x array.

C. R_x Tracking Algorithm

As shown in Fig. 9, T_x array could be considered as a black box, where k is the output of the black box and the input of the black box is the coordinate of T_x in T_x array. A discrete negative feedback control system could be designed to obtain the maximal k by adjusting the coordinate of T_x coil through the deviation ratio between k_{opt} and k. Activating an arbitrary T_x coil and putting a R_x onto this T_x coil. Then detecting k with a suitable frequency and recording k_{opt} at initial time. When R_x moves away from initial T_x coil, k would decrease. Then gain G could be calculated.

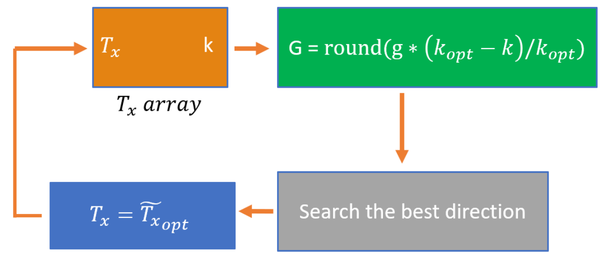

Fig. 9. R_x tracking algorithm (g is the amplification factor).

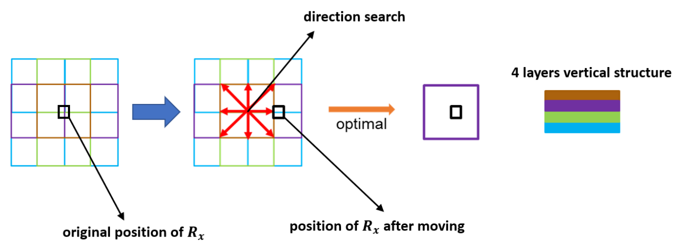

Fig. 10. Optimal direction searching on a 4-layer square T_x array.

Fig. 10 shows the complete process of optimal direction searching, where 4 layers vertical structure shows each layer in a 4-layer square T_x array. Firstly, a R_x coil located at the centre of T_x array with coordinate $T_x = (x, y)^{\mathsf{T}}$. As R_x moves away from the current T_x and to the right, the algorithm will try eight directions, centred on the current T_x coordinates $T_x = (x, y)^{\mathsf{T}}$, as the system is not able to determine the position of R_x. These directions are represented by vectors (including remaining stationery):

$$\text{dir} = \left\{ \begin{array}{c} \begin{pmatrix} -1 \\ -1 \end{pmatrix}, \begin{pmatrix} -1 \\ 0 \end{pmatrix}, \begin{pmatrix} 0 \\ -1 \end{pmatrix}, \begin{pmatrix} 1 \\ 1 \end{pmatrix} \\ \begin{pmatrix} 1 \\ 0 \end{pmatrix}, \begin{pmatrix} 0 \\ 1 \end{pmatrix}, \begin{pmatrix} 1 \\ -1 \end{pmatrix}, \begin{pmatrix} -1 \\ 1 \end{pmatrix}, \begin{pmatrix} 0 \\ 0 \end{pmatrix} \end{array} \right\} \quad (5)$$

Then, an attempt in each direction gives a new T_x coordinate $\tilde{T}_x[i]$ where $i = 1 \sim 9$.

$$\tilde{T}_x[i] = T_x + G * \text{dir}[i] \quad (6)$$

The algorithm measures k for each $\tilde{T}_x[i]$ and records them as $k[i]$. Then finding an optimal $\tilde{T}_x[i]$ and updating a new T_x coordinate:

$$\widetilde{T}_{x_{opt}} = \underset{\tilde{T}_x[i]}{\operatorname{argmin}} \left(\left(k_{opt} - k[i] \right) / k_{opt} \right) \quad (7)$$

$$T_x = \widetilde{T}_{x_{opt}} \quad (8)$$

New T_x will be fed into T_x array (black box) again to track moving R_x. This algorithm is performed by an external microcontroller, and it is necessary to build effective communication between the T_x array system and the microcontroller.

III. Results

The R_x tracking algorithm was implemented into the Raspberry Pi and simulated the 4-layer T_x array using Simulink. A connection was built between Simulink and Raspberry Pi.

The Raspberry Pi acted as a feedback controller of T_x array which received k from the 4-layer T_x array in Simulink and then sent T_x coordinate back to it, as shown in Fig. 11.

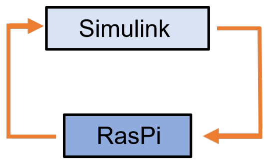

Fig. 11. Raspberry Pi acted as a feedback controller.

T_x and R_x are all PCB square coil. TABLE I gives the specification of T_x and R_x, where we assumed these T_x coils formed an unbounded T_x array. An initial coordinate of T_x was set and then the R_x was placed in the centre of initial T_x. Then R_x was moving freely on 4-layer T_x array. The moving speed on X-axis was set as $0.01 \sim 0.02\,m/s$; the moving speed on Y-axis was set as $(\pm)\,0.01 \sim 0.02\,m/s$, which means R_x would move in a positive X-axis direction but up and down direction randomly on Y-axis as shown in Fig. 12(d). g in Fig. 9 was set as 3.2. Fig. 1 was the WPT topology in this test and load was $3\,\Omega$ working under resonant frequency. D between T_x and R_x was $5\,cm$.

TABLE I
COIL SPECIFICATION (T_x IS ONE ELEMENT IN T_x ARRAY).

	T_x	R_x
d_o	100 mm	33.3 mm
d_i	85 mm	24.9 mm
w	2.5 mm	1.2 mm
s	7.5 mm	0.8 mm
n	1 turn	2 turns

Fig. 12 shows the test results within $50\,s$. By implementing R_x tracking algorithm with 4-layer T_x array, k could be maintained around k_{opt} with a small variation (0.007) instead of decrease to zero in the dynamic WPT system (Fig. 12(a)). However, there exist extremely short periods of oscillations in such a process which has been enlarged in Fig. 12(c) ($<\ 200\,ms$). These were caused by the optimal direction searching process as each $\tilde{T}_x[i]$ was turned on to measure k during the searching period. But due to the extremely short direction searching time at a suitable k sampling frequency, the periods of oscillations are also very short, which means that if we connect a large capacitor in parallel at the load side, these oscillations would hardly affect the normal operation of the load. Fig. 12(b) shows that stable and maximal PTE could be achieved in a dynamic WPT system by applying our method.

IV. Conclusion

To achieve maximal and stable PTE in dynamic WPT, a 4-layer T_x array system with R_x tracking algorithm has been proposed to track randomly moving R_x. We also discussed the coupling factor stability advantages of 4-layer T_x array system. Meanwhile, the tolerance of short-period oscillations was also illustrated. Through simulation experiments, we demonstrated

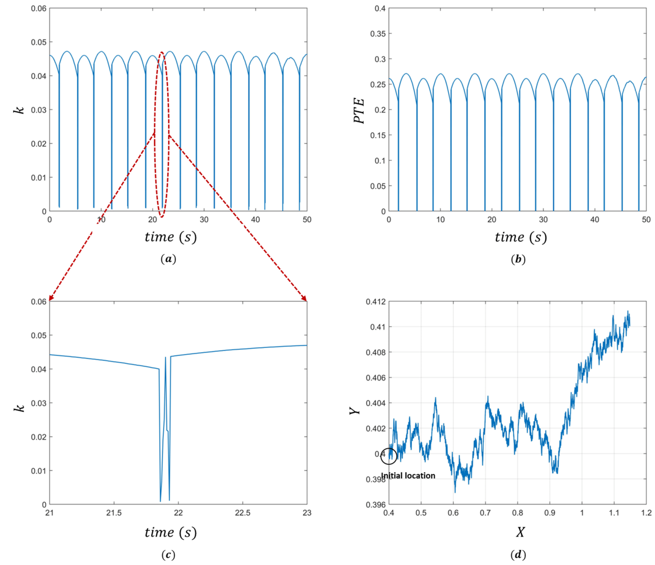

Fig. 12. (a) k vs time within 50 s; (b) PTE vs time within 50 s; (c) enlargement of direction searching oscillation from 21 s to 23 s; (d) trajectory of moving R_x within 50 s (m).

that the R_x tracking algorithm is effective, and the 4-layer T_x array can provide a stable coupling factor k (ignore oscillations), thereby achieving stable and maximum PTE. The size of T_x array depends on the moving area of R_x. For a small moving area, the cost is acceptable. Overall, the combination of 4-layer T_x array system and R_x tracking algorithm could provide a stable maximal PTE efficiently, which is a new implementation for the power supply of moving load devices.

References

[1] M. Schormans, V. Valente and A. Demosthenous, "Practical inductive link design for biomedical wireless power transfer: A tutorial," IEEE Transactions on Biomedical Circuits and Systems, vol. 12, no. 5, pp. 1112-1130, 2018.
[2] P. Alan, "Self-resonance in coils and the self-capacitance myth," Payne : Self Resonance in Coils, vol. 6, pp. 1–11, 2014.
[3] F. C. Flack, E. D. James, and D. M. Schlapp, "Mutual inductance of air-cored coils: Effect on design of radio-frequency coupled implants," Med. Biol. Eng., vol. 9, no. 2, pp. 79–85, Mar. 1971.
[4] C. Zierhofer and E. Hochmair, "Geometric approach for coupling enhancement of magnetically coupled coils," IEEE Trans. Biomed. Eng., vol. 43, no. 7, pp. 708–714, Jul. 1996.
[5] M. Ruhul Amin and R. B. Roy, "Design and simulation of wireless stationary charging system for hybrid electric vehicle using inductive power pad in parking garage," The 8th International Conference on Software, Knowledge, Information Management and Applications (SKIMA 2014), 2014, pp. 1-5.
[6] U. Jow and M. Ghovanloo, "Design and optimization of printed spiral coils for efficient transcutaneous inductive power transmission," IEEE Transactions on Biomedical Circuits and Systems, vol. 1, no. 3, pp. 193-202, 2007.
[7] K. Hata, T. Imura and Y. Hori, "Simplified measuring method of kQ product for wireless power transfer via magnetic resonance coupling based on input impedance measurement," IECON 2017 - 43rd Annual Conference of the IEEE Industrial Electronics Society, 2017, pp. 6974-6979.
[8] Y. Liu, R. Mai, D. Liu, Y. Li and Z. He, "Efficiency optimization for wireless dynamic charging system with overlapped DD coil arrays," IEEE Transactions on Power Electronics, vol. 33, no. 4, pp. 2832-2846, April 2018.